Lasers in Eng., Vol. 19, pp. 317–330
Reprints available directly from the publisher
Photocopying permitted by license only

Laser Surface Cladding of EN19 Steel with Stellite 6 for Improved Wear Resistance

D. GUPTA[1], B. L. MORDIKE[2], S. SHARIFF[3], G. PADMANABHAN[3], I. MANNA[1] AND J. DUTTA MAJUMDAR[1,*]

[1]*Department of Metallurgical and Materials Engineering, Indian Institute of Technology Kharagpur, West Bengal – 721302, India.*
[2]*Institut für Werkstoffkunde und Werkstofftechnik, Technische Universität Clausthal, Agricolstrasse 6, D-38678 Clausthal-Zellerfeld, Germany.*
[3]*Centre for Laser Processing of Materials (CLPM), ARCI, Hyderabad, Andhra Pradesh, India.*

The present study concerns the generation of a wear resistant Stellite 6 CO_2 laser clad layer on the surface of an EN19 steel substrate by means of laser surface cladding. Laser surface cladding was carried out by melting the Stellite powder (particle size 10 to 40 μm) supplied through a pneumatically driven powder delivery system (using a 4 MP powder unit) with a 9 kW continuous wave (CW) CO_2 laser with the wavelength 10.6 μm. The microstructure of the clad layer was found to consist of three zones: a clad layer comprised of dendrites of Stellite 6; an alloyed zone comprised of a cellular microstructure, which was a mixture of Fe and Co; and the heat affected zone (HAZ), which was a mixture of pearlite and martensite. Compared to the EN19 steel substrate, the micro-hardness of the clad layer represented a significant improvement, increasing to 1200 VHN.

Keywords: steel, silicon carbide, stellite, direct laser cladding, hardness, corrosion

1 INTRODUCTION

Surface microstructure and composition play a crucial role in determining the properties of a component. Surface treatment aims at a modification of the surface microstructure and/or composition of the near surface region of a component without influencing the bulk [1]. In order to improve the wear resistance the surface is covered with a hard and thick layer commonly known

*Corresponding author: Tel: +91 3222 283288; Fax: +91 3222 282280;
E-mail: jyotsna@metal.iitkgp.ernet.in

as hard-facing [1]. Weld overlaying, flame and plasma spraying are the commonly used surface treatment techniques to develop wear resistant coatings on metallic substrates [1]. Laser cladding is a process where a high power laser beam is used as a source of heat to melt the coating material and subsequently overlay it on the surface of the substrate with minimum dilution at the interface [2–4].

The original specific intention of laser cladding is to improve the local surface properties of metallic machine parts [1]. The ability to deliver a large power density (10^3 to 10^5 W/cm^2), high heating/cooling rates (10^3 to 10^5 K/s) and solidification speeds (1 to 30 m/s) are the notable advantages associated with laser surface cladding [2–4]. Laser cladding can be used to apply a layer of wear resistant coating on a metallic substrate. Conde *et al.* [5] developed a uniform and crack free boride containing a Ni hard-facing coated by laser cladding using a high power diode laser on plane carbon steel with an improved microhardness. d'Oliveira *et al.* [6] compared the high temperature behaviour of a Stellite 6 hard-faced layer on an AISI 304 stainless steel substrate. Though the laser cladding exhibited a superior hardness at low temperature, the PTA coating showed better thermal stability than the laser clad. Li *et al.* [7] reported that the laser surface cladding of a Co–Cr–W–Ni–Si alloy +20% SiCp on an IF steel substrate enhanced wear resistance and, the addition of SiC was found to be beneficial in enhancing it further. Navas *et al.* [8] compared the characteristics and properties of a NiCrBSi layer clad on a mild steel substrate by laser cladding and flame spraying, followed by surface flame melting. Manna *et al.* [9] developed a clad surface on an AISI 1010 steel substrate with Fe–B–C, Fe–B–Si and Fe–BC–Si–Al–C of bulk metallic glass composition. Although an amorphous layer was not retained in the microstructure, a significant improvement in the wear resistance was nevertheless achieved and the composition corresponding to a maximum improvement in the wear resistance was established.

Co-based super-alloys are popular as a hard-facing alloy applied to improve the wear resistance of mechanical parts, especially in hostile environments [10]. Stellite is a Co-based wear resistant super-alloy which was developed originally with a Co-Cr composition; it has since been modified by the addition of elements such as W, Mo, Si and Fe [10]. Stellite 6 is an alloy normally used on turbine blades because it offers very good wear and erosion resistance due to its high hardness and good bonding strength with the substrate [11, 12]. Ocelik *et al.* [13] developed a thick Co-based coating on cast iron by means of laser cladding with a side nozzle. A correlation between the processing conditions and the coating properties was undertaken. Frenk *et al.* [14] carried out detailed experimental and theoretical studies on the laser cladding of mild steel with Stellite 6 using a 1.5 kW continuous wave (CW) CO_2 laser to understand the effect of powder feed rate and scan speed on the clad height and mass efficiency. The process window for achieving the desired clad height was established.

In this work an attempt has been made to develop a wear resistant Stellite 6 clad layer on the surface of an EN19 steel substrate. A detailed characterization of the clad layer was undertaken and correlated with the laser parameters to optimize the process parameters. Finally, the wear resistance properties of the clad layer were evaluated and compared with the as-received EN19 steel substrate.

2 EXPERIMENTAL PROCEDURES

EN19 steel was used as the substrate for the experiments conducted in this work. The EN19 steel substrate dimensions were $20 \times 20 \times 5$ mm^3. Stellite 6 in powder form (composition (wt.%) Co: 62.1, Ni: 1.13, W: 3.96, Fe: 1.7, Cr: 28.9 and Si: 0.8) with a particle size ranging from 10 to 40 μm was used as a precursor for cladding.

Cladding was carried out by feeding Stellite 6 powder into the beam of a CO_2 laser through a pneumatically driven powder delivery system (using a 4 MP powder unit). The laser used was a 9 kW CO_2 laser (ML-108; MLI Laser, Inc.) operated in CW mode and emitting at a wavelength of 10.6 μm with a spot diameter of 2 mm. The powder feed was maintained at constant rate of 22 g/min. Cladding was carried out using Ar as a shroud gas at a pressure of 10 psi. A 10 to 25% overlap was applied between the successive clad tracks in order to have a uniform clad height and a homogeneous clad surface. The main process variables associated with laser surface cladding were varied: power; scan speed; powder feed rate; nozzle stand off; nozzle angle and shroud gas pressure. The experimental set-up used is shown in Fig. 1. To optimize the laser cladding processing parameters a large number of experimental trials were conducted under the set of lasing parameters given in Table 1. Following

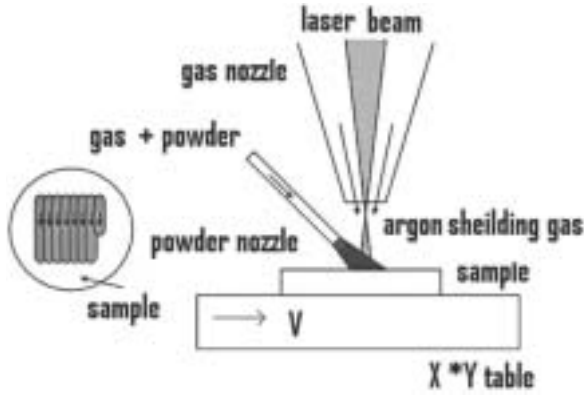

FIGURE 1
Schematic diagram of the laser surface cladding technique used.

Sl. No.	Parameters	Range
1	Laser power	2 to 4 kW
2	Focus distance	Focus to defocus +6 mm
3	Scan speed	5 to 30 mm/sec
4	Powder feeding rate	20 to 40 gm/min
5	Nozzle stand off	9 to 17 mm
6	Nozzle angle with horizontal	45 to 70°
7	Shroud gas type and pressure	Ar pressure from 5 to 10 psi

TABLE 1
Summary of the laser parameters used.

1	Number of revolution for each reading	200
2	Time taken in each reading	60 sec
3	Load used for testing	5 kg
4	Sand falling speed	206.79 +/− 10 gm/min
5	Hardness of rubber wheel	A58 to A62 Durometer
6	Sand	Rounded quartz grain sand by AFS 50/70 test sand
7	Motor for rotating wheel	200 +/− 10 rpm

TABLE 2
Details of the experimental parameters used in the abrasive wear testing.

laser cladding the microstructures of the clad layer (both the top surface and the cross-section) were characterized optically and with scanning electron microscopy (SEM). A detailed examination of the phases and compositions present within the clad layer was carried out with x-ray diffraction (XRD) and energy dispersive x-ray (EDX) analysis, respectively. The micro-hardness of the clad layer (both the top surface and along the cross-sectional plane) was measured by with a Vickers micro-hardness tester (HMV-2; Shimadzu, Corp.) using a 100 g applied load. Finally, the wear behaviour of the surface clad was compared to that of the as-received EN19 steel substrate by abrasive wear testing using a dry sand rubber wheel abrasion tribometer test rig (TR-50: CETR, Inc.). The conditions used for the abrasion testing are summarized in Table 2 During testing the specimens were pressed against the dry sand rubber wheel of a specified hardness and rotated at a fixed rotational speed with a preset force of 5 kg exerted by means of a leaver arm. The abrasive silica particles were between the test specimen and the rotating dry sand rubber wheel. The rotation of the dry sand rubber wheel was such that its contact force

moved in a direction opposite to the sand flow. The lever arm axis was placed such that it was approximately tangential to the dry sand rubber wheel surface and normal to the direction in which the load was applied. The specimens were cleaned ultrasonically with acetone and weighed before and after the test and the loss in weight was calculated. This procedure was repeated several times in order to obtain a steady state abrasion wear rate of the clad layer.

3 RESULTS AND DISCUSSION

3.1 Characteristics of the clad zone

The size and shape of a clad play an important role in determining the durability and properties of the coating. Figure 2 shows the size and shape of a single track laser clad layer of Stellite 6 on the EN19 steel substrate. From Fig. 2 it is evident that the clad layer formed on the surface is continuous, defect free, well adherent to the surface and consists of three different regions: the clad zone, an alloyed zone and the heat affected zone (HAZ). The height/width of the clad and depth of the alloyed zone and HAZ were found to vary with the laser parameters. Melting of a section of the substrate and its intermixing with the clad material leads to the formation of alloyed layers, the extent of which depends on the heat extraction towards the substrate during the solidification of clad metal. The formation of the alloyed zone, though essential to have a strong interfacial bond, is ideally kept to a minimal as dilution is undesirable when a clad layer has to be formed on the surface. A wide track width (with a large track width to overlap ratio maintaining uniform thickness) and thick

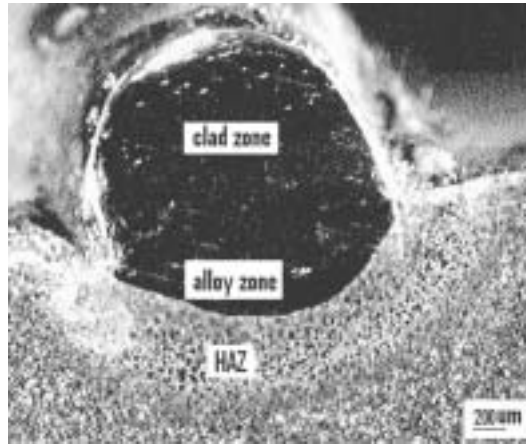

FIGURE 2
SEM micrograph showing the shape of a single track clad layer on the surface of the EN19 steel substrate laser clad with Stellite 6 (A laser power of 2 kW, a scan speed of 10 mm/s, a spot diameter of 2mm, a powder feed rate of 22 g/min and an Ar shroud gas at a pressure of 10 psi were used).

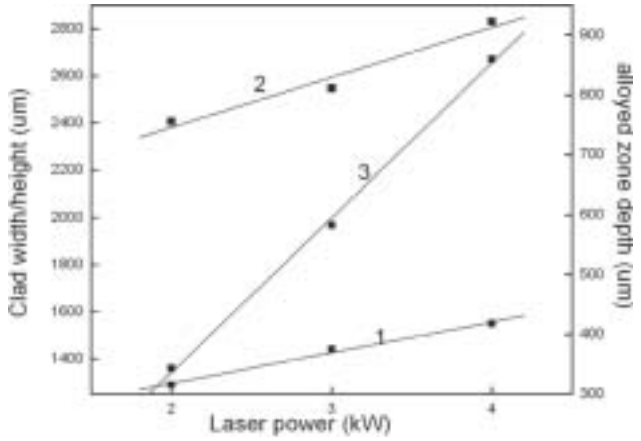

FIGURE 3
Variation of clad width (plot 1), clad height (plot 2) and alloyed zone width (plot 3) against applied laser power on the surface of the EN19 steel substrate laser clad with Stellite 6 (A scan speed of 10 mm/s, a spot diameter of 2 mm, a powder feed rate of 22 g/min and an Ar shroud gas at a pressure of 10 psi were used).

clad zone is beneficial in enhancing the performance of the deposited surface. Hence, laser parameters (laser power and scan speed) should be carefully chosen to yield a thick and uniform clad zone with the minimum number of tracks. In this regard it is relevant to mention that susceptibility to crack formation is frequently observed during the laser cladding of Stellite [15]. The propensity for crack formation was reportedly decreased by pre-heating of a Cr steel substrate and suppressed when pre-heated above 650 °C; however, the wear and corrosion properties were found to deteriorate with increasing pre-heating temperature due to diffusion of Fe from the substrate into the coating [16]. As one can see from Fig. 2, laser cladding under the present set of optimal parameters suppressed the formation of cracks. Figure 3 plots the effect of the applied laser power on the clad width, the clad height and the alloyed zone width of the laser clad Stellite 6 on the EN19 steel substrate. From Fig. 3 it is clear that the clad height, clad width and alloyed zone width increased with an increase in the applied laser power. Furthermore, the effect of the applied laser power on the alloyed zone width appears to be significant. The depth of the alloyed zone was found to vary from 300 to 1300 μm, with a variation of the dilution at the interface ranging from 28 to 35%. Increasing the laser power increases the quantity of energy transferred during the process and hence, the quantity of powder rendered molten during cladding results in an increased width and height of the clad zone. The observed increase in depth of the alloyed zone as the applied laser power increased can be attributed to the increased dilution resulting from the increased energy available for melting the substrate, which in turn leads to increased intermixing.

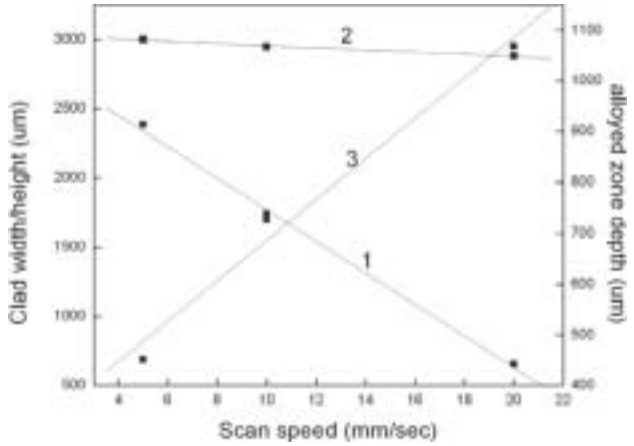

FIGURE 4
Variation of clad width (plot 1), clad height (plot 2) and alloyed zone width (plot 3) against scan speed on the surface of the EN19 steel substrate laser clad with Stellite 6 (A laser power of 2 kW, a spot diameter of 2 mm, a powder feed rate of 22 g/min and an Ar shroud gas at a pressure of 10 psi were used).

The variation of the clad width, clad height and alloyed zone width against the scan speed for laser clad Stellite 6 EN19 steel surface is shown in Fig. 4. It can be seen in Fig. 4 that the clad width and height decrease with an increase in the scan speed. This observed decrease in the clad width and clad height with increasing scan speed is probably due to a reduction in the quantity of powder delivered as a result of the increased scan speed leading to a lower interaction time (since interaction time = beam diameter/scan speed). The increase in the depth of the alloyed zone as the scan speed increases is due to the higher heat input to the substrate owing to a reduced amount of heat available for melting the clad layer. In this regard it is relevant to mention that the parameters chosen in the present study were optimal and led to the formation of a defect free and homogeneous clad layer. In the experimental trials conducted it was found that at very low powers it was not possible to form a clad layer and the application of very high power leads to excessive melting, porosity and crater formation in the clad layer.

Figure 5 shows the SEM micrographs of the clad zone, the alloyed zone and the HAZ of the laser clad Stellite 6 on the EN19 steel substrate. The microstructure of the clad zone consisted of dendrites of the Co-based super-alloy with precipitates of very fine complex carbides of Fe, Cr, Ni and W. Increases in applied laser power and decreases in the scan speed were found to increase the inter-dendrite spacing. Furthermore, the morphology of the clad zone was found to change from dendritic to equiaxed by the application of very high laser power. The microstructure of the alloyed zone can be seen in Fig. 5 to be predominantly equiaxed with the presence of a few ferrite grains

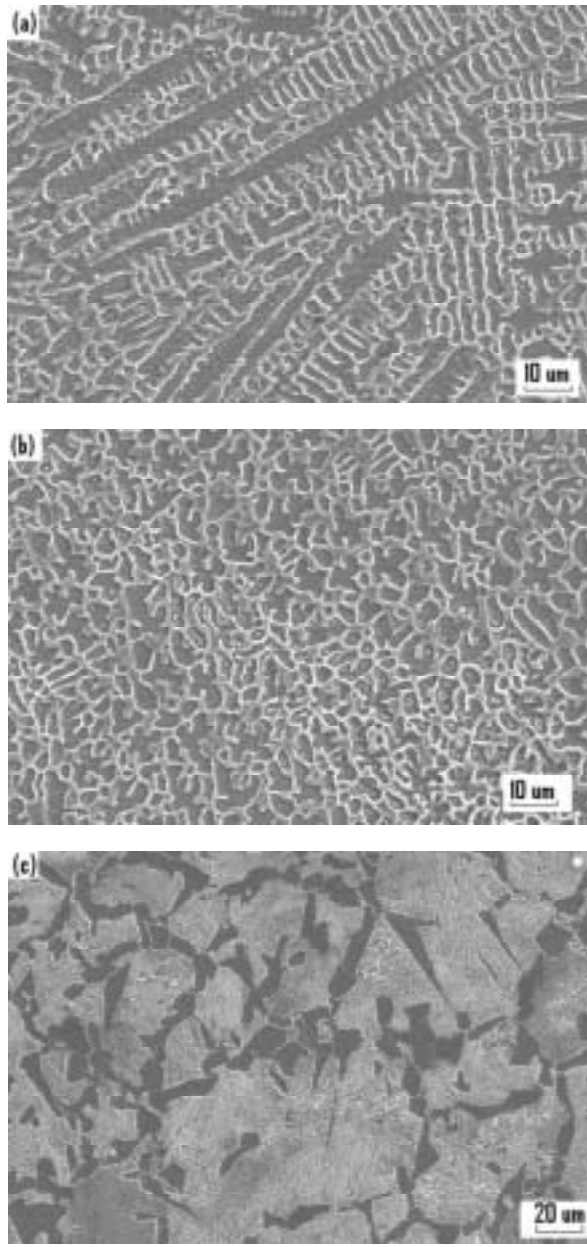

FIGURE 5
SEM micrographs of (a) the clad zone, (b) the alloyed zone and (c) the HAZ of the surface of the EN19 steel substrate laser clad with Stellite 6 (A laser power of 3.5 kW, a scan speed of 10 mm/s, a spot diameter of 2 mm, a powder feed rate of 22 g/min and an Ar shroud gas at a pressure of 10 psi were used).

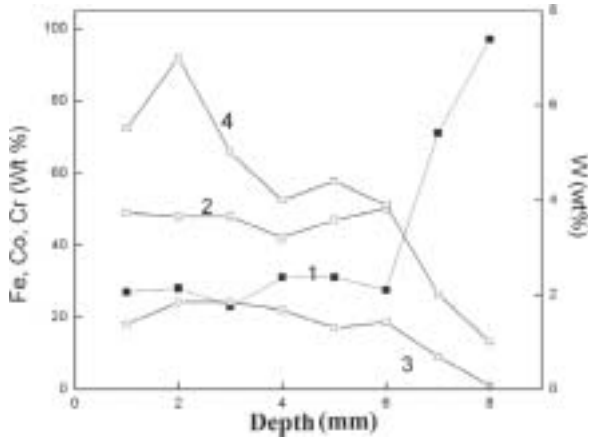

FIGURE 6
Elemental distribution of Fe (plot 1), Co (plot 2), Cr (plot 3) and W (plot 4) with the depth from the surface of the EN19 steel substrate laser clad with Stellite 6 (A laser power of 3.5 kW, a scan speed of 10 mm/s, a spot diameter of 2 mm, a powder feed rate of 22 g/min and an Ar shroud gas at a pressure of 10 psi were used).

in the microstructure. The HAZ can be seen to consist of very fine pearlite structures, a few Cr carbides and small amount of martensite. The volume fraction of pearlite was much higher than the as-received EN19 steel substrate.

A detailed EDX analysis of the clad zone, alloyed zone and HAZ was carried out to understand the variation of the composition of the laser clad Stellite 6 layer through to the EN19 steel substrate is shown in Fig. 6. One can from Fig. 6 that the clad zone was enriched with Co, Cr, W and Fe. Although the elemental content of Fe in the Stellite 6 clad powder is only 1.7%, after laser cladding the Fe content present in the clad is approximately 20 to 30%. This increased Fe content in the laser clad layer confirms that dilution from the substrate could not be suppressed during the laser cladding process. The W content can be seen from Fig. 6 to be at the maximum of 7 wt% in the near surface region of the laser clad, where after it decreased gradually to the minimum value of 1 wt% in the EN19 steel substrate. In the alloyed zone the Co and Cr content can be seen to decrease while the Fe content increases. This graded compositional distribution achieved in the clad zone is beneficial in reducing the residual stress distribution and enhancing the toughness of the clad. A similar trend was also observed when the laser clad was generated with different laser parameters.

Figure 7 shows the XRD profile obtained on the surface of the laser clad Stellite 6 layer on the EN19 steel substrate. From Fig. 7 it is evident that there are presence of complex carbides of Fe, Cr, Co, Ni and W ($M_{23}C_6$), inter-metallics of Co and W (Co_7W_6, Co_3W) and small amounts of Co in the microstructure. The presence of such elements is in agreement with other work reported on this system [10–12].

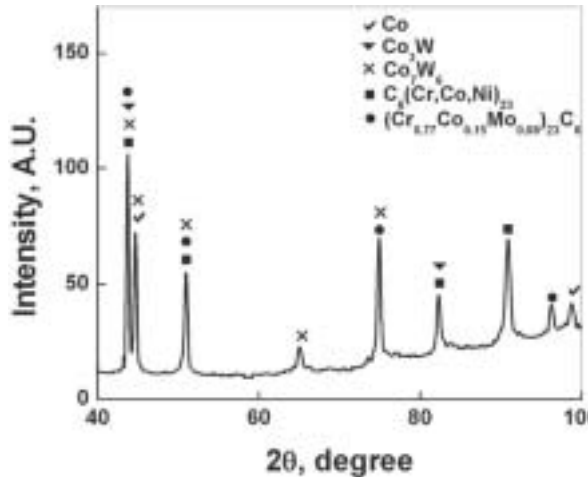

FIGURE 7
XRD profile of the surface of the EN19 steel substrate laser clad with Stellite 6 when processed with a laser power of 3 kW, a scan speed of 8 mm/s, a spot diameter of 2 mm, a powder feed rate of 22 g/min and an Ar shroud gas at a pressure of 10 psi.

3.2 Properties of the clad layer

A detailed micro-hardness analysis of the laser clad layer and the overlap zone was undertaken. In Fig. 8 the variation of the micro-hardness is shown as a function of depth from the surface of the laser clad layer. It can be seen in Fig. 8 that for the sample clad using an applied laser power of 3 kW, the micro-hardness of the laser clad layer surface was markedly higher than that of the EN19 steel substrate: 1000 VHN compared to 300 VHN, respectively. In the alloyed zone the micro-hardness was found to be less than at the surface at 900 VHN. This decrease in the micro-hardness of the alloyed zone can be attributed to the substantial dilution that took place as a result of the melting of substrate. The micro-hardness of the clad layer increased further when the applied laser power was increased to 3 kW (see Fig. 8, plot 2). This was possibly due to the higher power inducing greater levels of grain refinement in the laser clad layer. Figure 9 shows the effect of the applied laser power on the micro-hardness distribution on the laser clad layer, the alloyed zone and HAZ. From Fig. 9 significant increases in the micro-hardness of the clad layer and alloyed zone are discernible with an increase in the applied laser power. This observed increase in the micro-hardness of the clad layer and the alloyed zone with an increase in applied laser power is likely brought about by grain refinement associated with the higher cooling rate effected by the increased melting induced by the higher applied laser power. The hardness of the HAZ, however, can be seen from Fig. 9 to only increase marginally as the applied laser power is increased. It is therefore reasonable to conclude that whereas the mechanism of hardening in the clad layer and the alloyed zone

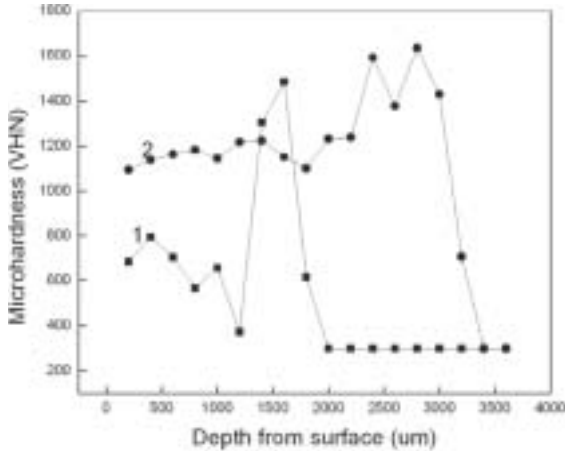

FIGURE 8
Variation of the micro-hardness as a function of depth from the surface through the laser clad layer of the surface of the EN19 steel substrate laser clad with Stellite 6 when processed with a laser power of 3 kW (plot 1) and 3.5 kW (plot 2), a scan speed of 10 mm/s, a spot diameter of 2 mm, a powder feed rate of 22 g/min and an Ar shroud gas at a pressure of 10 psi.

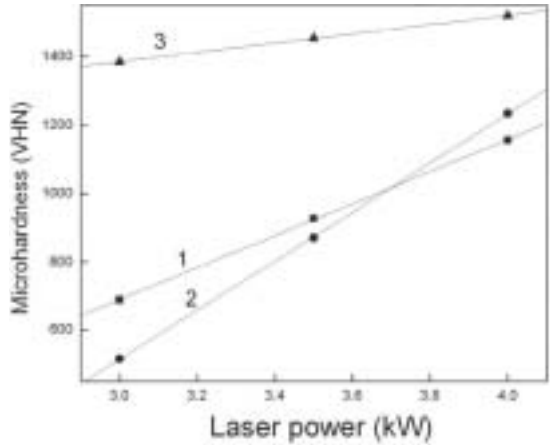

FIGURE 9
Effect of the applied laser power on the micro-hardness distribution of the clad layer (plot 1), alloyed zone (plot 2) and HAZ (plot 3) of the surface of the EN19 steel substrate laser clad with Stellite 6 when processed with a scan speed of 8 mm/s, a spot diameter of 2 mm, a powder feed rate of 22 g/min and an Ar shroud gas at a pressure of 10 psi.

is mainly the result of grain refinement and the presence of precipitates of carbides and inter-metallics, the mechanism of hardening in the HAZ is due to the martensitic transformation along with precipitation of carbides.

The wear behaviour of the EN19 steel substrate was studied by means of a dry sand rubber wheel abrasion test. Figure 10 gives the kinetics of wear as a

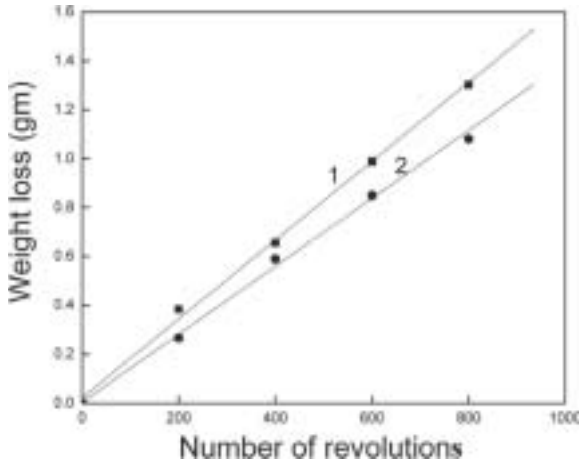

FIGURE 10
Kinetics of wear (in terms of cumulative vertical displacement) as a function of time for the as-received EN19 substrate (plot 1) and the laser clad Stellite 6 layer when processed with a laser power of 3 kW, a scan speed of 8 mm/s, a spot diameter of 2 mm, a powder feed rate of 22 g/min and an Ar shroud gas supplied at 10 psi. (plot 2).

function of time for the as-received EN19 substrate and the laser clad Stellite 6 layer. It is evident from Fig. 10 that the wear rate remains almost constant for both the EN19 substrate and the laser clad Stellite 6 layer, indicating that the mechanism of wear was predominantly abrasive in nature. Notably, there is a marginal improvement in wear resistance of the laser clad Stellite 6 layer (see Fig. 10, plot 2) when compared to the as-received EN19 substrate (see Fig. 10, plot 1). In addition, the wear rate was found to vary with laser parameters. This variation in wear behaviour of the laser clad Stellite 6 layer for different laser parameters is possibly due to differences in the microstructures and mechanical properties occasioned by the different laser parameters. The marginal improvement in wear resistance of the laser clad Stellite 6 layer, in contrast to the significant improvement in micro-hardness, is in all likelihood due to the formation of a brittle phase in the microstructure that subsequently lead to a higher rate of wear despite contributing to very high micro-hardness.

4 CONCLUSIONS

The detailed study of the laser surface cladding of Stellite 6 on an EN19 steel substrate has resulted in the following conclusions being made:

1. Laser surface cladding with the optimal laser processing parameters lead to the formation of a defect free and homogeneous clad layer whose width and height varied with the laser parameters.

2. The microstructure of the clad layer consisted of fine dendrites containing complex carbides of Fe, Cr, Co, Ni and W ($M_{23}C_6$), intermetallics of Co and W (Co_7W_6, Co_3W) and small amounts of Co.
3. The micro-hardness of the laser clad layer of Stellite 6 was improved significantly in comparison with the as-received EN19 steel substrate, with a maximum micro-hardness of 1200 VHN and 300 VHN, respectively.
4. A marginal improvement in the wear resistance was observed due to laser cladding of a Stellite 6.

ACKNOWLEDGEMENTS

The financial support for this work came from: the Council of Scientific and Industrial Research (CSIR), New Delhi; the Department of Science and Technology (DST), New Delhi and the Board of Research on Nuclear Science (BRNS), Bombay and is gratefully acknowledged.

REFERENCES

[1] Budinski K.G. *Surface Engineering for Wear Resistance*. New York: Prentice Hall. 1988.

[2] Molian P.A. and Sudarshan T.S. *Surface Modification Technologies – An Engineer's Guide*. New York: Marcel Dekker. 1989.

[3] Cahn R.W., Haasan P. and Kramer E.J. *Materials Science and Technology*. Weinheim: VCH 1989, p. 111.

[4] Rehn L.E., Picraux S.T. and Wiedersich H. *Surface Alloying by Ion, Electron and Laser Beams*. Metals Park: ASM. 1987. p. 1.

[5] Conde A., Zubiri F. and de Damborenea J. Cladding of Ni–Cr–B–Si coatings with a high power diode laser, *Materials Science and Engineering A: Structural Materials Properties Microstructure and Processing* **334**(1–2) (2002), 233–238.

[6] d'Oliveira, A.S.C.M., Vilar, R.M. and Feder C.G. High temperature behaviour of plasma transferred arc and laser Co-based alloy coatings. *Applied Surface Science* **201**(1–2) (2002), 154–160.

[7] Li M.-X., He Y.-Z. and Sun G.-X. Laser cladding Co-based alloy/SiCp composite coatings on IF steel. *Materials & Design* **25**(4) (2004), 355–358.

[8] Navas C., Colaço R., De Damborenea J. and Vilar R.M. Abrasive wear behaviour of laser clad and flame sprayed-melted NiCrBSi coatings. *Surface & Coatings Technology* **200**(24) (2006), 6854–6862.

[9] Manna I., Majumdar J.D. Ramesh C.B., Nayak S. and Dahotre N.B. Laser surface cladding of Fe–B–C, Fe–B–Si and Fe–BC–Si–Al–C on plain carbon steel. *Surface & Coatings Technology* **201**(1–2) (2006), 434–440.

[10] Betteridge W. *Cobalt and its Alloys*. Chichester: Ellis Horwood. 1982. pp. 61–119.

[11] So H., Chen C.T. and Chen Y.A. Wear behaviours of laser-clad Stellite alloy 6. *Wear* **192**(1–2) (1996), 78–84.

[12] de Hosson J.T.M. and de mol van Otterloo L. Surface engineering with lasers: Application to Co based materials. *Surface Engineering* **13**(6) (1997), 471–481.

[13] Ocelík V., d'Oliveira U., de Boer, M. and de Hosson, J.T.M., Thick Co-based coating on cast iron by side laser cladding: Analysis of processing conditions and coating properties. *Surface & Coatings Technology* **201**(12) (2007), 5875–5883.

[14] Frenk A., Vandyoussef, M., Wagnière J-D., Kurz W. and Zryd A. Analysis of the laser-cladding process for Stellite on steel. *Metallurgical and Materials Transactions* **B28**(3) (1997), 501–508.

[15] Wulin S., Echigoya J., Beidi Z., Changsheng X. and Kun C. Effects of Co on the cracking susceptibility and the microstructure of Fe–Cr–Ni laser-clad layer. *Surface & Coatings Technology* **138**(2–3) (2001), 291–295.

[16] Jendrzejewski R., Navas C., Conde A., de Damborenea J.J. and Sliwinski G. Properties of laser-cladded Stellite coatings prepared on preheated chromium steel. *Materials & Design* **29**(1) (2008), 187–192.